

FIG. 3. Two-dimensional flow diagram for incident and reflected elastic shocks. Shock incidence and reflection results in streamlines  $S_1$ ,  $S_2$ , and  $S_3$  giving a surface rotation  $\delta_1 + \delta_2 + \delta_3$ .

velocity<sup>8</sup> as

$$u_2^2 = (A_2/A_1)^2 u_1^2, \quad (5)$$

and

$$u_3^2 = (B_2/A_1)^2 (\phi/\Psi) u_1^2. \quad (6)$$

$A_2/A_1$  is the amplitude ratio of the reflected compressional wave to the incident compressional wave.  $B_2/A_1$  is the amplitude ratio of the reflected shear wave to the incident compressional wave.  $C_p$  and  $C_s$  are velocities for the compressional and shear waves respectively in

$$\phi[(U_{app}^2/C_p^2) - 1]^{1/2} = \tan(\pi/2 - e), \quad (7)$$

and

$$\Psi = [(U_{app}^2/C_s^2) - 1]^{1/2} = \tan(\pi/2 - f). \quad (8)$$

The angle  $e$  is the angle between the free-surface and the incident compressional wave. The angle  $f$  is the angle between the free-surface and the reflected shear wave. The amplitude ratios are

$$\frac{A_2}{A_1} = \frac{4\mu\phi\Psi - (\Psi^2 - 1)[\lambda + \phi^2(\lambda + 2\mu)]}{4\mu\phi\Psi + (\Psi^2 - 1)[\lambda + \phi^2(\lambda + 2\mu)]} \quad (9)$$

and

$$\frac{B_2}{A_1} = \frac{-4\mu\phi[\lambda + \phi^2(\lambda + 2\mu)]}{4\mu^2\phi\Psi + (\Psi^2 - 1)[\lambda + \phi^2(\lambda + 2\mu)]} \quad (10)$$

where  $\lambda$  and  $\mu$  are Lamé constants.

The optical lever deflection can be related to the particle velocity  $u_1$  by extending the flow diagram of a hydrodynamic shock described in Ahrens and Gregson. This extension (see Fig. 3) will not depend upon the usual approximation that the free-surface velocity is twice the particle velocity. Instead, the optical lever deflection is equated to the surface rotations produced by each of the three shocks

$$1/2ad^{-1} = \delta_1 + \delta_2 + \delta_3, \quad (11)$$

where  $\delta_1$ ,  $\delta_2$ , and  $\delta_3$  are the rotations associated with the incident compressional shock, the reflected dilatational shock, and the reflected shear stress shock respectively.

<sup>8</sup> W. M. Ewing, W. S. Jardetzky, and F. Press, *Elastic Waves in Layered Media* (McGraw-Hill Book Company, Inc., New York, 1957), Chap. 2, Sec. 2-1.

From the geometry of Fig. 3,

$$\delta_1 = \tan^{-1}[u_1 \cos e / (U_{app} - u_1 \sin e)]. \quad (12)$$

The surface rotation of the reflected compressional rarefaction is

$$\delta_2 = \tan^{-1}\{u_2 \cos(e + \delta_1) / [S_1 - u_2 \sin(e + \delta_1)]\}, \quad (13)$$

where the streamline  $S_1$  has a magnitude

$$S_1 = [(U_{app} - u_1 \sin e) / \cos \delta_1]. \quad (14)$$

The surface rotation of the reflected shear stress rarefaction is

$$\delta_3 = \tan^{-1} \left[ \frac{u_3 \cos(\pi/2 - f - \delta_1 - \delta_2)}{S_2 - u_3 \sin(\pi/2 - f - \delta_1 - \delta_2)} \right], \quad (15)$$

where the streamline  $S_2$  has a magnitude

$$S_2 = \{[S_1 + u_2 \sin(e + \delta_1)] / \cos \delta_2\}. \quad (16)$$

Equations (5) to (16) are used in a digital computer program to find values of  $u_1$ , the incident compressional shock particle velocity. The necessary elastic wave velocities, material constants, and apparent velocity are used to calculate the amplitude ratios relating particle velocities  $u_2$  and  $u_3$  to  $u_1$ . Values of  $u_1$  are selected and used in Eqs. (12) to (16) until Eq. (11) is valid to the numerical precision required in the experiment. Such values are 5% to 10% less than particle velocities computed by the free-surface approximation.

An additional feature to consider in this experiment that does not concern a plane wave or a two-dimensional steady-state experiment is an impact off the optic axis of the optical lever alignment. Figure 4 illustrates the geometry of this case. Assume an off-axis impact

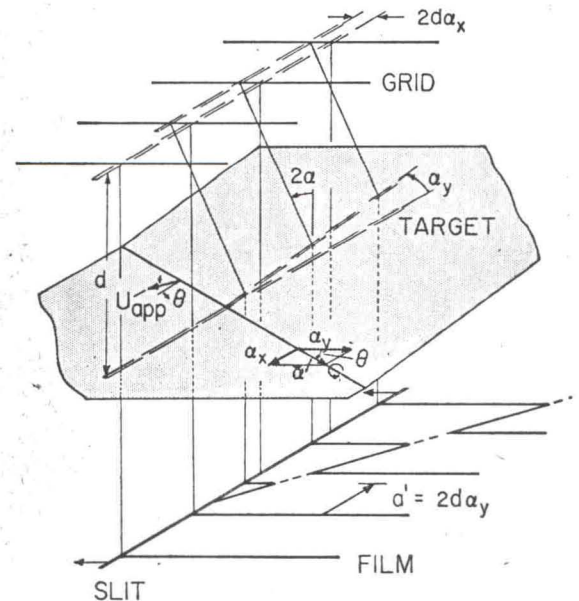


FIG. 4. Geometry of an off-axis impact.